Received: 18 April 2021 | Revised: 28 May 2021 | Accepted: 4 June 2021

DOI: 10.1002/jbio.202100129

FULL ARTICLE

JOURNAL OF BIOPHOTONICS

Dependence of laser-induced optical breakdown on skin type during 1064 nm picosecond laser treatment

Hyeonsoo Kim[1] | **Jewan Kaiser Hwang**[2] | **Jongman Choi**[1,3] | **Hyun Wook Kang**[1,4*]

[1]Industry 4.0 Convergence Bionics Engineering, Pukyong National University, Busan, Republic of Korea

[2]Mymirae Research Institute for Dermatologic Science, Seoul, Republic of Korea

[3]Research and Development, Bluecore Company, Busan, Republic of Korea

[4]Department of Biomedical Engineering, Pukyong National University, Busan, Republic of Korea

***Correspondence**
Hyun Wook Kang, Department of Biomedical Engineering, Pukyong National University, Busan 48513, Republic of Korea.
Email: wkang@pukyong.ac.kr

Funding information
Ministry of SMEs and Startups, Grant/Award Number: S2780486

Abstract

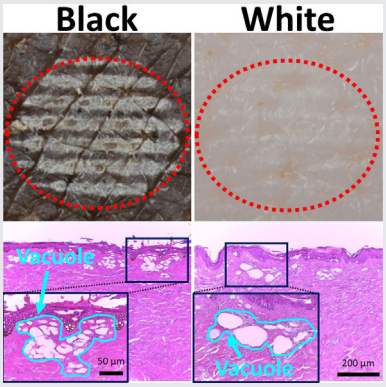

The current study aims to evaluate the dependence of laser-induced optical breakdown (LIOB) on skin types by using 1064 nm picosecond laser with micro-lens arrays (MLA) and diffractive optical elements (DOE). Both black and white skin tissues were examined to comparatively assess the LIOB effects in the skin in terms of laser-induced vacuolization. The black skin irradiated at 3.0 J/cm^2 demonstrated that MLA yielded a deeper distribution (180-400 μm) of laser-induced vacuoles with a size of 67 μm, compared to DOE (180-280 μm; 40 μm in size). However, the white skin presented that MLA created larger vacuoles (134 μm in size) in a smaller number at deeper distributions (125-700 μm) than MLA with the black skin. DOE generated no laser-induced vacuolization in the white skin. The white skin tissue with inherent higher scattering could be responsible for deeper vacuolization after the picosecond laser treatment. Further investigations are expected to determine the optimal treatment conditions for various skin types.

KEYWORDS

diffractive optical elements, fitzpatrick skin type, laser-induced optical breakdown, micro-lens arrays, picosecond laser skin treatment

1 | INTRODUCTION

Melasma, also known as chloasma (when occurs in pregnancy), is a common pigmentary disease that occurs to hyperpigmentation in the epidermis and dermis of the skin [1]. The disease happens in protruding face areas, such as cheeks, upper lip, and forehead, which can be easily exposed to the sunlight [1–5]. Melasma is typically accompanied by dark discoloration (brown, gray, and black) patches on the skin and happens in all the races and regions [6]. The causing factors of melasma are thought to be exposure to ultra-violet (UV) light in sunlight, agglomeration of melanin in skin, gravidity, genetic

Abbreviations: CIE, international commission on illumination; DOE, diffractive optical elements; FWHM, full width at half maximum; LIOB, laser-induced optical breakdown; MLA, micro-lens arrays; UV, ultra-violet.

vulnerability, and hormonal malfunction [6–8]. However, the exact pathogenesis of melasma still remains unexplored [9]. Melasma mainly occurs in Fitzpatrick skin types IV-VI as the Fitzpatrick scale is a system to classify skin type, based upon the amount of melanocyte in the skin and the skin's reaction to sunlight exposure [8]. However, Fitzpatrick skin types I-III also can easily undergo melasma because of the high UV sensitivity [10].

Picosecond laser treatment has been adopted as a suitable method for treating pigmented skin disease because of non-invasiveness and rapid recovery time [11, 12]. A picosecond laser pulse width (hundreds of 10^{-12} s) generates high pressure (2 GPa) and high temperature (2000-4000 K) through multiphoton ionization in skin [13]. Furthermore, both high pressure and high temperature entail plasma expansion along with generation of shockwaves, which is called laser-induced optical breakdown (LIOB), leading to vacuolization inside the skin [14]. The laser-induced vacuolization caused by LIOB destroys melanin in the epidermal and dermal layers with no or minimal thermal damage and induces collagen regeneration inside the vacuole, resulting in scar-free skin recovery [15, 16]. To reduce unwanted thermal injury, micro-lens arrays (MLA) and diffractive optical elements (DOE) are clinically employed with a picosecond laser system [17–19]. Typically, MLA has a Gaussian-like micro-beam distribution whereas DOE has a flat-like micro-beam distribution [19]. Owing to the inherent optical features, either lens is selected by the condition of the melasma. For instance, MLA is used to treat deep darkish melasma located in the dermal layer while DOE is employed to remove the light-colored melasma, that is, widely distributed in the skin. In spite of successful removal of melasma, the clinical outcomes of the picosecond laser treatment often depend on skin type [20].

The current study aimed to comparatively evaluate the dependence of LIOB effects on two different skin types categorized as Fitzpatrick skin types I and VI after irradiation of 1064-nm picosecond laser with MLA and DOE at two different radiant exposures (H_0 in J/cm^2). We hypothesized that bright-colored skin with low melanin index and high scattering could create larger vacuoles in deep dermis of the skin than dark-colored skin, under the same condition. Two types ex vivo porcine skin tissues (black and white) were tested with a 1064 nm picosecond laser system in conjunction with MLA and DOE to compare distributions and locations of the laser-induced vacuoles in the skin layers. Histological analysis was performed to evaluate depth, size, and distribution of the laser-induced vacuoles under the basal membrane in a quantitative manner.

2 | EXPERIMENTAL

2.1 | Light source

For LIOB experiments, a 1064 nm picosecond Nd:YAG laser system (pulse width = 450 ps at full width at half maximum [FWHM]; Picore, Bluecore Company, Busan, Republic of Korea) was used in conjunction with MLA (fused silica, macro-beam diameter = 4 mm in circular shape, micro-beam diameter = 220 μm, 37 micro-beams, focal length = 40 mm; Bluecore Company, Busan, Republic of Korea) and DOE (fused silica, macro-beam size = 4 mm in rectangular shape, micro-beam diameter = 165 μm, 49 micro-beams, focal length = 40 mm; Bluecore Company, Busan, Republic of Korea). Both MLA and DOE were applied to fractionate the incident macro-beam and to maximize the light intensity for laser-induced vacuolization in skin after LIOB. Two radiant exposures (H_0 = 3.0 and 6.0 J/cm^2) were employed from MLA and DOE to compare the extent of the laser-induced vacuolization in black and white skin tissues. The corresponding micro-beam energy was 10.3 and 20.5 mJ/micro-beam for MLA (macro-beam energy/pulse = 0.38 and 0.76 J) and 9.8 and 19.6 mJ/micro-beam for DOE (macro-beam energy/pulse = 0.48 and 0.96 J) in order to deliver the equal radiant exposure to the target tissue. Based on the preliminary study [21], the focal depth was 35 mm (from lens to target tissue) in order to generate the laser-induced vacuolization under the basement membrane with no or minimal damage on the tissue surface. The laser light emitted from MLA and DOE at 3.0 J/cm^2 were also irradiated on the black-colored dimming paper to compare spatial beam distributions by evaluating power density from individual micro-beams.

2.2 | Ex vivo experiments

For ex vivo experiments, minipig skin tissues (Cronex M-pig; age: 6 months; weight: 30-65 kg) of black and white colors were procured from CRONEX Corp. (Seoul, Republic of Korea). The current study inevitably used one pig for each skin type to maintain the equivalent CIE value. The fresh skin samples (N = 5) were randomly harvested in a size of 45 cm^2 from the abdominal lesion of each minipig. Then, prior to testing, all the prepared samples were stored at 4°C in order to prevent physical deformation and to minimize dehydration. Before the experiments, an International Commission on Illumination (CIE) Lab color space test was conducted to quantify and compare perceptual lightness (L^*), red/green value (a^*), and blue/yellow value (b^*) of black and white skin tissues in order to classify skin color and to match with the Fitzpatrick skin type for consistency [22]. Each tissue

surface was photographed by using a digital camera. Image J (National Institute of Health, Bethesda, Maryland) was used to convert each acquired image to a binary image and then divided into three color Lab stack images to measure the Lab color values. The measured values were compared with a von luschan scale (categorized into 36 stages) to confirm the relevance of the tested skin types to Fitzpatrick skin types (I = 0-6, II = 7-13, III = 14-20, IV = 21-27, V = 28-34, and VI = 35-36) [23]. The current study evaluated the dependence of the LIOB effects on the skin type during 1064 nm picosecond laser irradiation. Thus, the two different skin colors (black and white) were tested to represent Fitzpatrick skin types VI and I [24]. Each tissue specimen was initially situated on a translational stage and laterally moved by 50 μm after irradiation of a single pulse. A total of 20 shots at each radiant exposure was applied to the skin (total treated length = 1 mm). Top-surface images were photographed to compare the spatial distributions of the micro-beam spots on the surface of each skin type.

2.3 | Histological analysis

Laser-irradiated tissues were harvested and fixed in 10% neutral formalin solution (Sigma Aldrich, St. Louis, Missouri) for 2 days. After the fixation, paraffin blocks were made and sliced by 5 μm in thickness to prepare six slides per paraffin block (N = 6). The sections were stained with hematoxylin and eosin (HE) for histological analysis. All the histology slides were imaged at ×100 and ×400 by using an optical microscope (Leica DM500, Leica, Wetzlar, Germany). Laser-induced vacuoles were identified by a pathologist and characterized in terms of shape, size, and position. The vacuoles were distinguished from sweat glands and follicles that have a hole-shaped structure in the skin tissue [25]. Image J was used to measure dimensions (depth and area) of laser-induced vacuoles inside the tissue. Vacuole coverage was also estimated to compare the vacuole distributions in the black and white tissues at various skin depths. For quantitative analysis, histology images were initially converted to binary images, and the threshold was set at ~ 20% to classify the laser-induced vacuoles. After the conversion, all the images were segmented by 40 μm height to quantify the vacuole areas as a function of skin depth. Then, the segmented images were calculated by dividing the area of the laser-induced vacuoles by a total tissue area. The Mann-Whitney U test was performed for non-parametric statistical analysis by using SPSS software 22 (SPSS Inc., Chicago, Illinois). $P < .05$ was considered statistically significant.

3 | RESULT

Figure 1 presents laser-induced responses of ex vivo porcine skin tissue to laser irradiation with MLA and DOE. Figure 1A shows a CIE Lab color space distribution of Fitzpatrick skin types that was determined by using a von luschan scale. The Fitzpatrick skin types had a wide distribution of the CIE Lab color values (L^* = 13-96, a^* = −3-18, and b^* = −6-39). Black skin had the CIE Lab color values of L^* = 29, a^* = 4.4, and b^* = 7.4, corresponding to the Fitzpatrick skin types V and VI (L^* = 13-28, a^* = 5.7-18, and b^* = − 6-20). On the other hand, white skin yielded the values of L^* = 70, a^* = 2.5, and b^* = 7.8, representing the Fitzpatrick skin types I and II (L^* = 96.4 ~ 96.5, a^* = − 0.4-0.03, and b^* = 4.8-5.9). It was noted that the L^*, a^*, and b^* values of the white skin were lower than those of the Fitzpatrick skin type possibly because of no blood flow

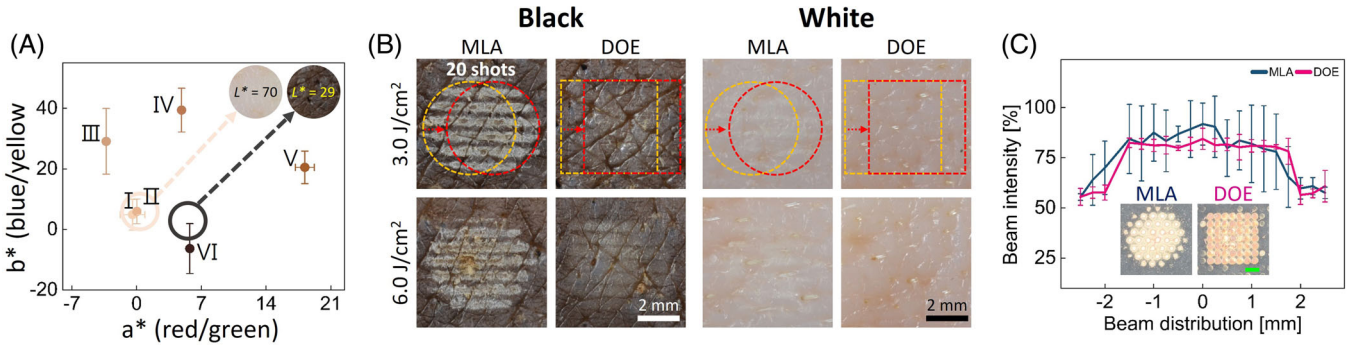

FIGURE 1 Comparison of ex vivo porcine skin tissues with different skin colors (black and white) after irradiations with micro-lens arrays (MLA) and diffractive optical elements (DOE) at H_0 = 3.0 and 6.0 J/cm^2: A, CIE Lab color space value (a^* = red/green; b^* = blue/yellow; L^* = perceptual lightness) distributions of Fitzpatrick skin types (I–VI) and tested skin tissues (circles), B, top-view images of laser-irradiated skin, and C, micro-beam images and beam distribution of MLA and DOE at 3.0 J/cm^2 (bar = 1 mm). Note that a macro-beam was moved from left (orange dashed lines) to right (red dashed lines) during the irradiation (lateral movement = 50 μm/pulse; total of 20 shots; bar = 2 mm; green bar = 1 mm)

after tissue extraction. Figure 1B displays the top-view images of the black and white skin surfaces after irradiation of 20 shots with MLA and DOE at 3.0 J/cm^2 (top) and 6.0 J/cm^2 (bottom). MLA produced macro-beam spots in a circular shape while DOE generated rectangular macro-beam spots. Figure 1C shows the beam distributions of MLA and DOE on the black-colored dimming paper ($H_0 = 3.0$ J/cm^2). MLA experienced a large deviation in the spot size with a high concentration of light intensity at the center. On the other hand, DOE yielded relatively uniform beam distributions. Regardless of lens type, the black skin clearly evidenced the overlapped macro-beam spots because of strong light absorption by dark-colored skin [26]. On the other hand, the white skin exhibited blurred or less noticeable traces of the macro-beam spots and thermal lesions after the irradiations with MLA and DOE.

Figure 2 shows HE-stained images of black and white skin tissues after laser irradiation with MLA and DOE at $H_0 = 3.0$ J/cm^2. In the case of the black skin, both MLA and DOE evidently created laser-induced vacuoles under the basal membrane. According to Figure 2A, MLA deeply distributed multiple small vacuoles from papillary dermis to reticular dermis in the black skin. Relatively larger and deeper vacuoles were observed in the white skin than the black skin (vacuole depth = 283 ± 114 μm for black vs 368 ± 171 μm for white; $P < .01$ and vacuole size = 67 ± 34 μm for black vs 134 ± 100 μm for white; $P < .001$; Figure 2A). On the other hand, DOE yielded relatively a less number of the smaller laser-induced vacuoles near the papillary dermis in the black skin (vacuole depth = 140 ± 62 μm; Figure 2B), compared to MLA. However, the white skin demonstrated photo-disrupted damage in the papillary dermis with no vacuolization.

Figure 3 displays HE-stained images of black and white skin tissues after laser irradiation with MLA and DOE at $H_0 = 6.0$ J/cm^2. For both black and white skin tissues, MLA and DOE generated vacuoles under the basal membrane. In Figure 3A, MLA yielded a deep distribution of the vacuoles in the black and white skin tissues. However, the white skin underwent photo-disruptive ablation at the upper epidermis and created relatively larger vacuoles than the black skin (ie, vacuole size = 70 ± 37 μm for black vs 162 ± 98 μm for white; $P < .001$). In Figure 3B, DOE yielded the laser-induced vacuoles adjacent to the papillary dermis in the black skin (vacuole depth = 210 ± 54 μm), which were smaller and less than MLA ($P < .001$). However, no laser-induced vacuolization was found in the white skin after the irradiation with DOE.

Figure 4 compares the numbers of laser-induced vacuoles in black and white skin tissues at various vacuole depths and H_0. According to Figure 4A, regardless of skin type, MLA created more vacuoles and showed a deeper range of axial vacuolization (from 160 to 550 μm), compared to DOE (from 160 to 280 μm). For the black skin, both MLA and DOE at 3.0 J/cm^2 generated the maximum

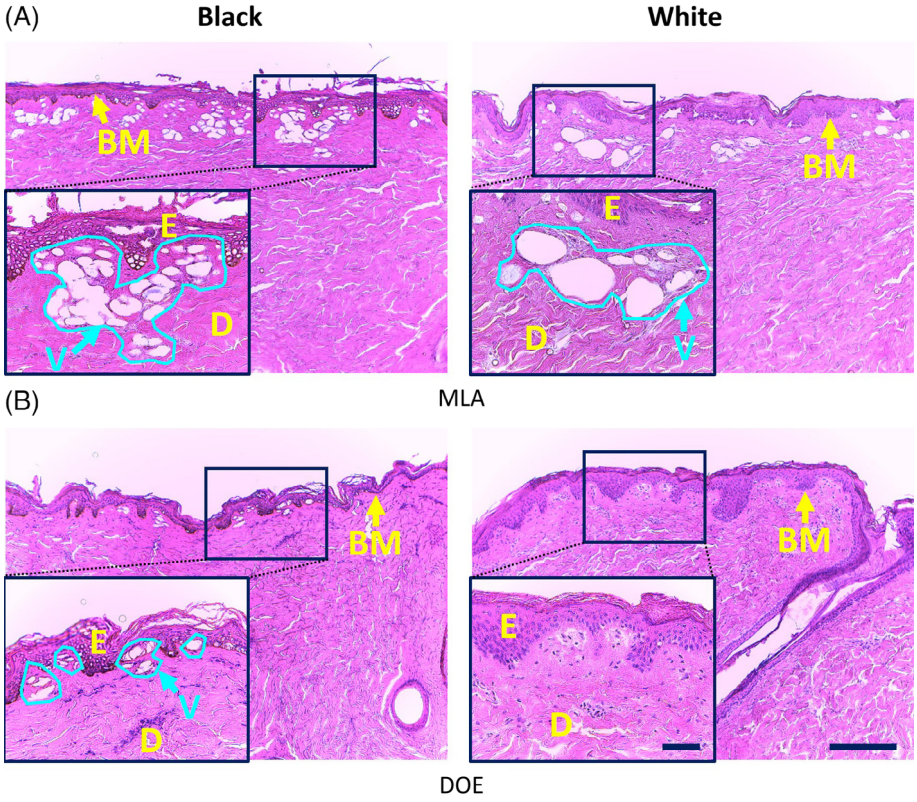

FIGURE 2 Histological images (HE-stained) of black (left column) and white (right column) porcine skin tissues after irradiation with A, micro-lens arrays (MLA) and B, diffractive optical elements (DOE) at $H_0 = 3.0$ J/cm^2 (100 and bar = 200 μm). Note that inlets (400 and bar = 50 μm) represent the magnified areas on the skin surface (black solid lines; E: epidermis, D: dermis, BM: basal membrane, and V: laser-induced vacuole)

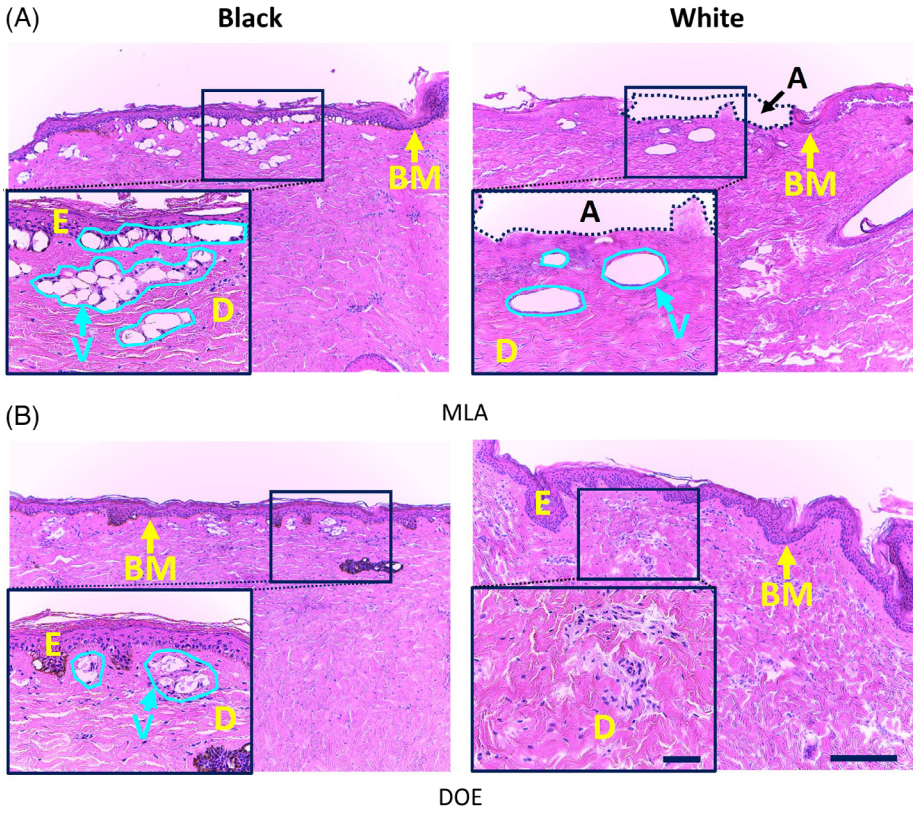

FIGURE 3 Histological images (HE-stained) of black (left column) and white (right column) porcine skin tissues after irradiation with A, micro-lens arrays (MLA) and B, diffractive optical elements (DOE) at $H_0 = 6.0$ J/cm^2 (100 and bar = 200 μm). Note that inlets (400 and bar = 50 μm) represent the magnified areas on the skin surface (black solid lines; E: epidermis, D: dermis, BM: basal membrane, and V: laser-induced vacuole)

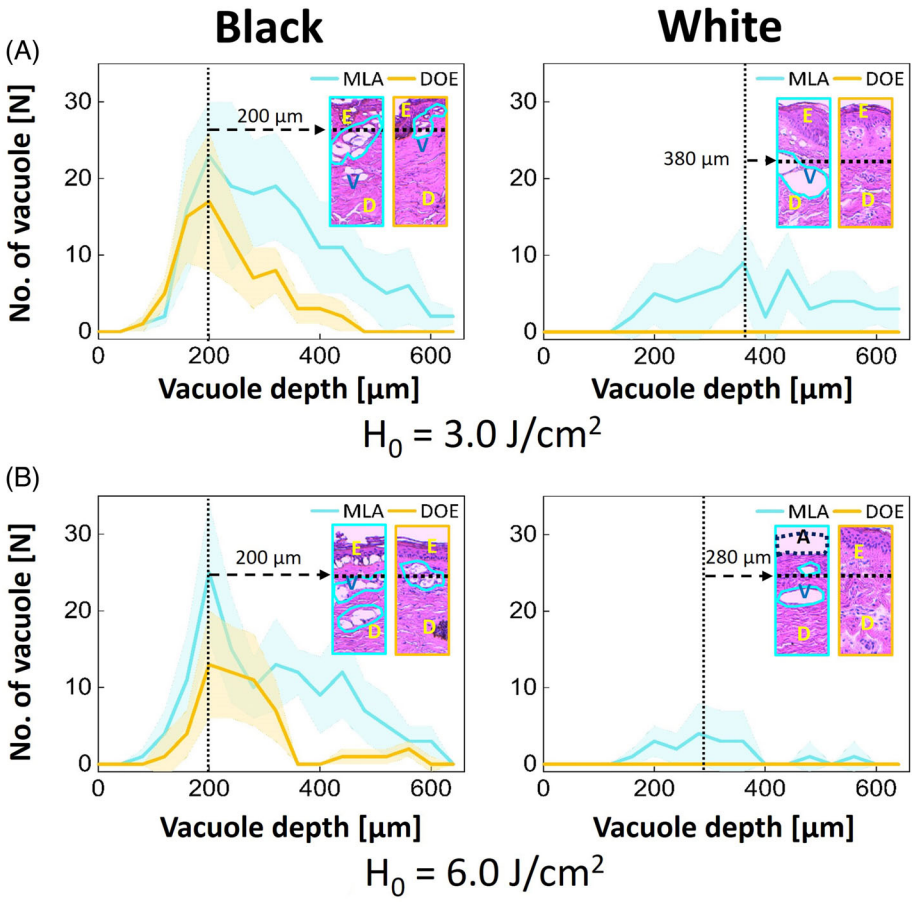

FIGURE 4 Quantitative analysis of black and white skin tissues after irradiation with micro-lens arrays (MLA) and diffractive optical elements (DOE) measured from histology images: comparison of number of vacuoles as function of vacuole depth generated at A, $H_0 = 3.0$ J/cm^2 and B, $H_0 = 6.0$ J/cm^2. Note that inlets (100) represent the vacuole distributions in the tissue (E: epidermis, D: dermis, V: laser-induced vacuole, and A: ablated region; filled area around line: SD)

number of the vacuoles at the depth of ~ 200 μm. On the other hand, the white skin after laser irradiation with MLA yielded deeper vacuolization (~ 200 μm for black vs ~ 380 μm for white) but a relatively small number of vacuoles, compared to the black skin (~ 110 for black vs ~ 60 for white; $P < .05$; Figure 4A). However, no or minimal vacuoles were observed after irradiation with DOE on the white skin. At $H_0 = 6.0$ J/cm^2, MLA and DOE produced the maximum number of the vacuoles at the depth of 200 μm for the black skin (Figure 4B). The higher H_0 induced insignificant changes in the average vacuole depth (vacuole depth $= 283 \pm 114$ μm for 3.0 J/cm^2 vs 294 ± 126 μm for 6.0 J/cm^2 in black skin; $P = .50$). On the other hand, the white skin generated a less number of the vacuoles after the irradiations with MLA and DOE.

Figure 5 quantifies the number of vacuoles as a function of vacuole size in black and white skin tissues after irradiations with MLA and DOE at $H_0 = 3.0$ and 6.0 J/cm^2. According to Figure 5A, both MLA and DOE at $H_0 = 3.0$ J/cm^2 generated the largest number of the vacuoles with a size of 70 μm in the black skin. MLA generated more vacuoles than DOE (~ 170 for MLA vs ~ 70 for DOE; $P < .05$). On the other hand, the larger vacuoles (average size $= 134 \pm 100$ μm) in a smaller number were found under the basal membrane in the white skin after the irradiation with MLA, compared to the black skin (Figure 5A). DOE induced photo-disruptive damage in the papillary dermis along with no laser-induced vacuolization. Figure 5B demonstrates that in spite of the higher H_0, both MLA and DOE yielded a less number of the laser-induced vacuoles with a size of 55-70 μm in the black skin. More vacuoles were created with MLA than DOE ($P < .05$). On the other hand, the white skin presented larger vacuoles in smaller number (vacuole size $= 162 \pm 98$ μm) generated by MLA. DOE yielded no laser-induced vacuolization in the white skin and accompanied photo-disruptive injury at the dermis.

Figure 6 presents laser-induced vacuole coverage as a function of tissue depth after irradiations with MLA and DOE on black and white skin tissues at $H_0 = 3.0$ and 6.0 J/cm^2. The vacuole coverage represents the relative spatial distributions of the vacuoles generated within the target skin area. In Figure 6A, both MLA and DOE at $H_0 = 3.0$ J/cm^2 generated most vacuoles under the basal membrane, irrespective of skin type. In the case of the black skin, MLA yielded a deeper coverage (180-400 μm) of the vacuoles, whereas DOE had a relatively narrower coverage (180-280 μm). MLA and DOE induced the maximum coverage of 22% at 360 μm and 17% at 260 μm, respectively. The average coverage was 14% for MLA and

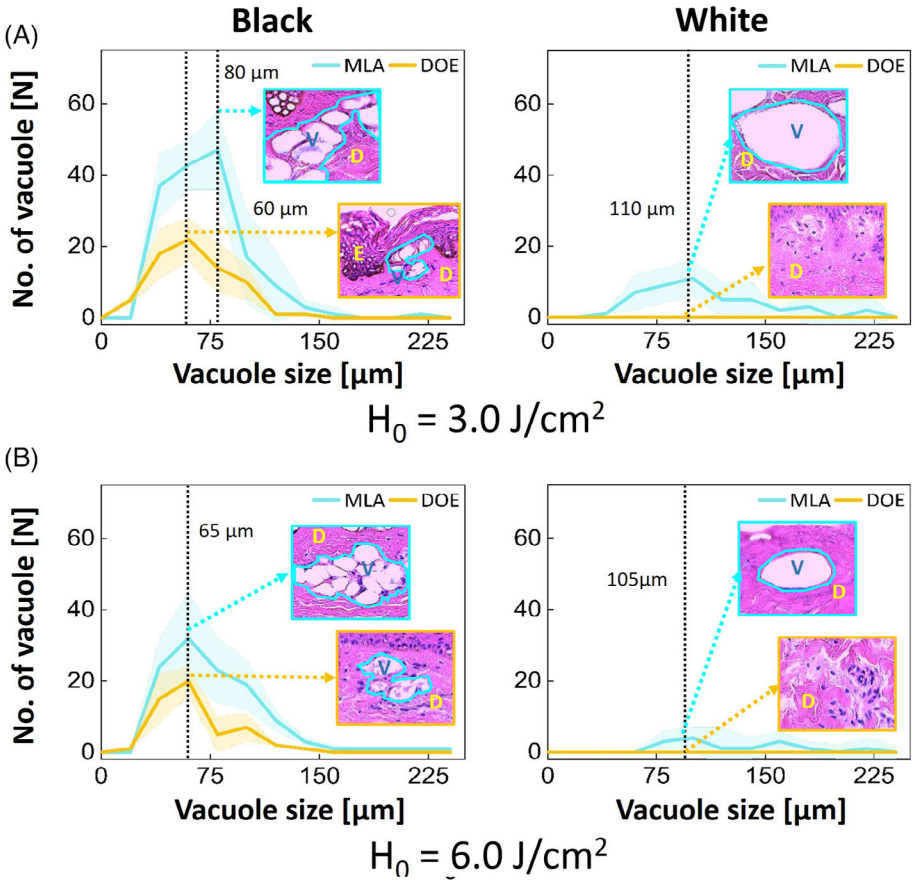

FIGURE 5 Quantitative analysis of black and white skin tissues after irradiation with micro-lens arrays (MLA) and diffractive optical elements (DOE) measured from histology images: comparison of number of vacuoles as function of vacuole size generated at A, $H_0 = 3.0$ J/cm^2 and B, $H_0 = 6.0$ J/cm^2. Note that inlets (400) represent the average vacuole size (E: epidermis, D: dermis, and V: laser-induced vacuole; filled area around line: SD)

6% for DOE. For the white skin, MLA created a smaller amount of the vacuoles in a deeper distribution (125-700 μm), in comparison to the black skin. The maximum vacuole coverage of 22% occurred at 460 μm (average coverage = 15%). On the other hand, DOE generated no laser-induced vacuolization (0% coverage) in the white skin. Figure 6B demonstrates the vacuole coverage after the irradiations with MLA and DOE at $H_0 = 6.0$ J/cm^2. In the case of the black skin, MLA had a deeper distribution of the vacuoles than DOE (ie, 180-550 μm for MLA vs 225-400 μm for DOE). MLA generated the maximum vacuole coverage of 24% at 360 μm, whereas DOE yielded the maximum coverage of 14% at 300 μm. The average coverage was 13.5% for MLA and 5.3% for DOE, which were higher than those at $H_0 = 3.0$ J/cm^2. For the white skin, MLA demonstrated photo-disruptive ablation in the epidermis and the papillary dermis, leading to a smaller amount of the vacuoles in a narrower distribution (125-750 μm) than the white skin irradiated at $H_0 = 3.0$ J/cm^2 (Figure 3A). The maximum vacuole

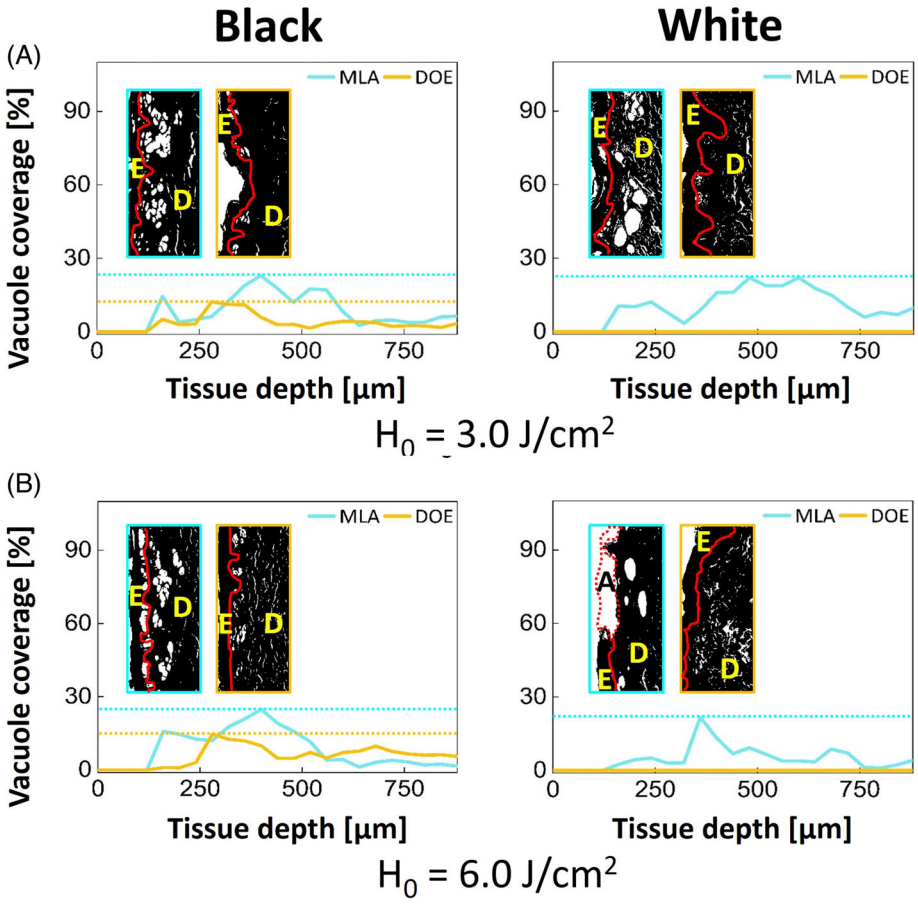

FIGURE 6 Quantitative comparison of vacuole coverage as function of tissue depth after irradiation with micro-lens arrays (MLA) and diffractive optical elements (DOE) on black and white skin tissues at A, $H_0 = 3.0$ J/ and B, $H_0 = 6.0$ J/cm^2. Note that inlets (100) represent binary images to classify vacuoles in the tissue (E: epidermis, D: dermis, red line: basal membrane, and A: ablated region)

TABLE 1 Correlation of laser-induced vacuolization with skin type, lens type, and H_0

Skin type	Lens type	H_0 (J/cm^2)	Vacuole depth (μm)	Vacuole size (μm)	Vacuole coverage (%)	Distribution range (μm)
Black	MLA	3.0	283 ± 114	67 ± 34	14	180–400
		6.0	294 ± 126	70 ± 37	14	180–550
	DOE	3.0	140 ± 62	40 ± 21	6	180–280
		6.0	210 ± 54	55 ± 24	6	225–400
White	MLA	3.0	368 ± 171	134 ± 100	15	125–700
		6.0	320 ± 82	162 ± 98	10	125 –750
	DOE	3.0	n/a	n/a	n/a	n/a
		6.0	n/a	n/a	n/a	n/a

Abbreviations: DOE, diffractive optical elements; MLA, micro-lens arrays.

coverage of 21% occurred at 375 μm (average coverage = 10%). In contrast, DOE still entailed no laser-induced vacuolization (0% coverage) in the white skin. Table 1 summarizes a correlation of the laser-induced vacuolization with skin color, radiant exposure, and lens type.

4 | DISCUSSION

Melasma treatment has been widely studied because of a high occurrence rate in various cultures and regions [27, 28]. Although the current clinical treatment mainly focuses on the location, size, and depth of the melasma, the laser treatment conditions need to be optimized for various skin types with different amounts of melanin. The aim of the current study was to evaluate the dependence of LIOB effects on two different skin types (black and white) by using 1064-nm picosecond laser light with MLA and DOE. A CIE Lab color space confirmed that the tested black- and white-colored skin tissues were categorized as Fitzpatrick skin types VI and I. The ex vivo porcine skin tissues barely reveals human skin properties in terms of blood flow, temperature, and water contents because of the after tissue extraction. Nevertheless, ex vivo skin showed a suitable value for the Fitzpatrick skin type. The black skin experienced the laser-induced vacuolization near the basal membrane (depth = 283 μm for MLA and 140 μm for DOE), creating a relatively uniform size of vacuoles (eg, 67 μm for MLA and 40 μm for DOE at 3.0 J/cm^2). On the other hand, the white skin irradiated with MLA created larger vacuoles in a smaller number at the deeper locations possibly due to high scattering features (depth = 368 μm and size = 134 μm for MLA at 3.0 J/cm^2; Figures 4-6). It was noted that DOE with smaller micro-beam energy generated no laser-induced vacuolization [18]. Figure 6 displays insignificant changes in the average vacuole coverage between the skin types whereas noticeable changes were found in the vacuole number, size, and distribution (Figures 4 and 5). The equivalent coverage between the skin types implicates that the white skin yielded larger vacuoles in a smaller number than the black skin. Conceivably, the black skin with higher melanin contents could achieve the immediate light absorption, generating LIOB in the tissue and the resultant vacuolization in the skin [26]. In contrast, the white skin with high specular reflection and scattering could contribute to less light absorption, eventually inducing weaker LIOB in the tissue. Although the higher radiant exposure was applied to overcome the weak LIOB, photo-disruptive damage occurred instead in both epidermis and papillary dermis (Figure 3).

Recently, a number of studies demonstrated the effect of LIOB on different skin types after picosecond laser treatment [20, 29]. Moustafa et al. examined Fitzpatrick skin types III and IV with 1064 and 532 nm picosecond laser lights (H_0 = 4 J/cm^2). Their results demonstrated that 11 to 16 weeks follow-ups yielded 100% clearance of pigmentation in skin type III patients and 75% clearance in skin type IV patients after the first treatment [20]. It is conceivable that the larger vacuoles created in the white skin (Figures 2, 3, and 5) could be responsible for more effective pigment removal and collagen regeneration, compared to the black skin. Nguyen et al. removed pigmented lesions in Fitzpatrick skin types III to IV by using 1064 nm laser at H_0 = 1.05 to 1.12 J/cm^2. The skin types III to IV yielded 75% to 90% clearance of the pigmentation in the tissue [29]. Typically, the melanin index in the skin plays as an important role in generating photodisruption [30]. A low melanin index along with high scattering features in the white skin could be responsible for more spatial distributions of the incident photons, widening the laser-induced vacuolization [31, 32]. Large vacuoles can effectively remove pigments from the skin. However, the large-sized vacuoles may cause a longer healing time for the skin than the small-sized ones due to collagen remodeling. Therefore, a less number of laser pulses could be applied to the white skin in order to have the equivalent LIOB effect and to reduce the size of the vacuoles.

The current study tested ex vivo porcine skin with two different colors to compare LIOB effects. Although white skin experimentally showed larger and deeper laser-induced vacuolization than black skin, human skin tissue may have different optical properties (absorption and scattering) because of no blood flow, water contents, and constant skin temperature. Thus, the inhomogeneous optical properties of the human skin tissue can vary the degree of the LIOB effects during 1064 nm picosecond laser treatment. Furthermore, the current study compared the responses of the two different skin types to the picosecond laser treatment by quantifying CIE Lab color values for the skin colors and the extent of laser-induced vacuoles. Regardless of radiant exposures, DOE presented no vacuolization in the white skin possibly due to lower micro-beam energy levels, compared to MLA [15, 33]. Various irradiation conditions, such as macro-beam size, focal depth, and radiant exposure should thus be optimized to maximize the laser-induced vacuolization in the bright-colored tissue. For clinical translations, further studies will be performed to assess the dependence of LIOB on multiple human skin types in terms of recovery time and melasma clearance.

5 | CONCLUSION

The current study demonstrated the spatial dependence of LIOB on different ex vivo porcine skin types by using

1064 nm picosecond laser light with MLA and DOE. High scattering and less superficial light absorption in white skin could entail larger laser-induced vacuoles in a smaller number at the deeper locations, compared to black skin. Further investigations will validate the current findings with various human skin types to warrant efficacy and safety for clinical applications.

ACKNOWLEDGMENTS

This work was supported by the Technology Development Program (S2780486) funded by the Ministry of SMEs and Startups (MSS, Korea). The authors appreciate Seyeon Park for her language editing.

CONFLICT OF INTEREST

The authors declare no potential conflict of interest.

DATA AVAILABILITY STATEMENT

The data that support the findings of this study are available from the corresponding author upon reasonable request.

ORCID

Hyeonsoo Kim https://orcid.org/0000-0002-0957-3716
Jongman Choi https://orcid.org/0000-0002-9295-7111
Hyun Wook Kang https://orcid.org/0000-0002-0861-1354

REFERENCES

[1] B. Iranmanesh, M. Khalili, S. Mohammadi, R. Amiri, M. Aflatoonian, *Dermatol. Ther.* **2021**, *34*, e14927.
[2] K. M. Babbush, R. A. Babbush, A. Khachemoune, *Int. J. Dermatol.* **2021**, *60*, 166.
[3] M. Rendon, M. Berneburg, I. Arellano, M. Picardo, *J. Am. Acad. Dermatol.* **2006**, *54*, S272.
[4] J. N. Mehrabi, E. Bar-Ilan, W. Shehadeh, A. Koren, L. Zusmanovitch, F. Salameh, G. Isman Nelkenbaum, T. Horovitz, E. Zur, T. S. Lim, *J. Cosmet. Dermatol.* **2021**, 1.
[5] A. Y. Lee, *Pigm. Cell Melanoma Res.* **2015**, *28*, 648.
[6] A. C. Handel, L. D. Miot, H. A. Miot, *Anais Brasileiros de Dermatologia* **2014**, *89*, 771.
[7] P. E. Grimes, *Arch. Dermatol.* **1995**, *131*, 1453.
[8] O. A. Ogbechie-Godec, N. Elbuluk, *Dermatol. Ther.* **2017**, *7*, 305.
[9] M. Bhura, S. Sharma, *Int. J. Health Clin. Res.* **2021**, *4*, 61.
[10] S. Del Bino, J. Sok, E. Bessac, F. Bernerd, *Pigm. Cell Res.* **2006**, *19*, 606.
[11] E. M. Graber, E. L. Tanzi, T. S. Alster, *Dermatol. Surg.* **2008**, *34*, 301.
[12] G. H. Fisher, R. G. Geronemus, *Dermatol. Surg.* **2005**, *31*, 1245.
[13] B. Varghese, V. Bonito, M. Jurna, J. Palero, M. Horton, R. Verhagen, *Biomed. Opt. Express* **2015**, *6*, 1234.
[14] P. K. Kennedy, D. X. Hammer, B. A. Rockwell, *Prog. Quant. Electron.* **1997**, *21*, 155.
[15] H. C. Lee, J. Childs, H. J. Chung, J. Park, J. Hong, S. B. Cho, *Sci. Rep.* **2019**, *9*, 4186.
[16] H. Kwon, S. Yang, Y. Cho, E. Shin, M. Choi, Y. Bae, J. Jung, G. H. Park, *J. Eur. Acad. Dermatol. Venereol.* **2020**, *34*, 2907.
[17] C. Y. Hwang, C. C. Chen, *Photodermatol., Photoimmunol. Photomed.* **2020**, *36*, 63.
[18] C. Kopp, L. Ravel, P. Meyrueis, *J. Opt. A: Pure Appl. Opt.* **1999**, *1*, 398.
[19] A. Krasnaberski, Y. Miklyaev, D. Pikhulya, L. Kleinschmidt, W. Imgrunt, M. Ivanenko, V. Lissotschenko in Efficient beam splitting with continuous relief DOEs and microlens arrays, Vol. 8236 (Ed. Eds.: Editor), International Society for Optics and Photonics, **2012**, pp. 823609.
[20] F. Moustafa, A. Suggs, S. S. Hamill, P. M. Friedman, *Lasers Surg. Med.* **2020**, *52*, 586.
[21] H. Kim, J. K. Hwang, M. Jung, J. Choi, H. W. Kang, *Biomed. Opt. Express* **2020**, *11*, 7286.
[22] I. L. Weatherall, B. D. Coombs, *J. Invest. Dermatol.* **1992**, *99*, 468.
[23] H. M. van Minderhout, M. V. Joosse, D. C. Grootendorst, N. E. Schalij-Delfos, *Strabismus* **2019**, *27*, 127.
[24] A. Treesirichod, S. Chansakulporn, P. Wattanapan, *Ind. J. Dermatol.* **2014**, *59*, 339.
[25] L. Habbema, R. Verhagen, R. Van Hal, Y. Liu, B. Varghese, *J. Biophotonics* **2012**, *5*, 194.
[26] S. Shah, T. S. Alster, *Am. J. Clin. Dermatol.* **2010**, *11*, 389.
[27] N. Neagu, C. Conforti, M. Agozzino, G. F. Marangi, S. H. Morariu, G. Pellacani, P. Persichetti, D. Piccolo, F. Segreto, I. Zalaudek, *J. Dermatol. Treat.* **2021**, 1.
[28] L. L. Zhou, A. Baibergenova, *Int. J. Dermatol.* **2017**, *56*, 902.
[29] H. T. Nguyen, E. V. Doan, T. N. Tran, T. T. Vu, H. N. Phan, J. F. Sobanko, *Lasers Surg. Med.* **2020**, 1.
[30] C. Goh, *J. Dermatol. Treat.* **2003**, *14*, 243.
[31] R. Pecora Vol. *1884*, Dynamic light scattering from macromolecules, International Society for Optics and Photonics, **1993**, pp. 2–15.
[32] V. V. Lyubimov, A. G. Murzin, V. B. Volkonski, A. B. Utkin in Vol. *2925*, statistical characteristics of photon paths and optimization of the tomography algorithms for the case of strongly scattering media, International Society for Optics and Photonics, **1996**, pp. 218–226.
[33] D. J. Kang, J. P. Jeong, B. S. Bae, *Opt. Express* **2006**, *14*, 8347.

How to cite this article: H. Kim, J. K. Hwang, J. Choi, H. W. Kang, *J. Biophotonics* **2021**, e202100129. https://doi.org/10.1002/jbio.202100129